

# The Effects of *in vitro* Target Compression Modulus on Laser Thrombolytic Ablation Rate

Abram D. Janis

Sean J. Kirkpatrick

Kenton W. Gregory

Scott A. Prah

Oregon Medical Laser Center, Portland, OR

## ABSTRACT

Laser thrombolysis is under investigation as a safe and rapid therapy for arterial recanalization in acute embolic stroke. Clot formation is a complex process affected by many factors that lead to differences in strength and hemoglobin concentration in samples formed from whole blood. The strength of thrombus formed *in vivo* also varies with age. Laser thrombolysis experiments were performed using a 577 nm 1  $\mu$ sec pulsed dye laser at an energy of approximately 25 mJ and a repetition rate of 4 Hz. Laser ablation and confined compression modulus were measured with three *in vitro* clot models: gelatin, static clot, and reconstituted clot. Laser ablation studies demonstrate that laser ablation efficiency ( $\mu$ g/mJ/pulse) is not significantly affected by differences in the confined compression modulus of clot. This agrees with previous studies using dye and gelatin. These results provide support for the effective use of this laser thrombolysis system for the removal of clots of varied age and strength.

**Keywords:** clot model, laser thrombolysis, stroke, ablation efficiency

## 1. INTRODUCTION

Laser thrombolysis is a potential treatment for stroke, which is the leading cause of morbidity and the third leading cause of mortality in the United States<sup>1</sup>. A stroke occurs when blood flow to the brain is interrupted, leading to ischemia and hypoxia. In the majority of cases this is caused by an embolic thrombus blocking flow through an artery. Earlier work using laser thrombolysis for the treatment of acute myocardial infarction<sup>2-4</sup> and pre-clinical studies in a swine cerebral thromboemboli model indicate that this therapy is a viable, highly selective, and safe treatment for the recanalization of certain cerebral arteries. Currently, this laser thrombolysis for is being tested in a clinical trial acute stroke therapy.

The neurological catheter (LaTIS, Minneapolis) delivers laser energy to the clot through a flexible fluid core catheter with an approximate diameter of 2 mm. The laser is coupled to a 200  $\mu$ m fused silica fiber, which carries the laser energy into the catheter. Angiographic contrast solution is continuously injected over the fiber at a rate of 4.2 mL/min. The fiber terminates 3-4 mm before the end of the catheter. The laser energy is carried to the occluding thrombus through the fluid, which cools the area of ablation, clears ablated particles, and is angiographically visible<sup>5</sup>, permitting the imaging of clot removal in real time.

Hemoglobin is the primary absorbing chromophore in thrombus and light is selectively absorbed by thrombus through most of the visible spectrum. The laser source is a 1  $\mu$ s pulsed dye laser emitting at 577 nm. At this wavelength, thrombus has a lower ablation threshold (20-30 mJ/mm<sup>2</sup>) than vessel tissue (1,100-1,500 mJ/mm<sup>2</sup> in saline, 250 mJ/mm<sup>2</sup> in blood)<sup>6</sup> due to a large difference in the absorption coefficient<sup>7</sup>.

*In vivo*, the mechanical properties of thrombus change as it is biochemically modified over time. Clinically, this may have implications for the performance of the LaTIS neuro catheter system. The potential variation in the range of mechanical properties of stroke causing clot targets was the motivation behind these experiments.

*Ex vivo* thrombus (static clot) formed by allowing whole blood to clot in tubing, is extremely variable<sup>14</sup>. This variation is possibly due to the complexity of the clotting cascade or the presence of the transglutaminase

Factor XIII. Both the mechanical properties and hemoglobin concentration varied between individuals and could not provide the required reproducibility.

Previous investigations have successfully measured the effects of altering laser parameters on red-dye gelatin phantoms while *in vitro* studies on thrombus are limited<sup>7-11</sup>. A reconstituted clot model was developed to provide a reproducible yet clinically relevant clot target in which the hemoglobin concentration is held constant and fibrinogen concentration has been controlled<sup>8,12</sup>. The mechanical properties of the model clot are the result of enzymatic reactions that mimic those found in the final common pathway of the clotting cascade *in vivo*, the conversion of fibrinogen to fibrin by the proteolytic enzyme thrombin in the presence of Calcium ion.

Previously, we have demonstrated that laser thrombolytic ablation efficiency was unaffected by clot ultimate strength in the range studied<sup>12</sup>. For the current studies, a confined compression test was designed. Three thrombus models were used to test the effects of varying the compression modulus of the *in vitro* target on laser thrombolytic ablation: gelatin with red dye, static clot, and reconstituted clot.

The goals of this study were to 1) measure the confined compression modulus of gelatin with red dye, static clot, and reconstituted clot models and 2) measure the effects of confined compression modulus on ablation efficiency ( $\mu\text{g}/\text{mJ}/\text{pulse}$ ). We hypothesized that increases in clot model stiffness, as measured by confined compression modulus, would decrease ablation efficiency.

## 2. MATERIALS AND METHODS

### 2.1. Gelatin Phantom

300 Bloom Gelatin (Sigma) was mixed with a 0.18% aqueous solution of Direct Red 81 (Sigma) in proportions of 5, 10, 15, and 20% gelatin (wt/wt). The mixtures were allowed to soak for 4 hr., then were heated to 65°C for 25 min. The solutions were injected into six 100 mL plastic beakers and IV tubing (Baxter, 2.5 mm ID). The samples were allowed to cure in a 10°C water bath for 18 hr. prior to testing. These methods were adapted from gelatin bloom strength measurement standards<sup>13</sup>.

### 2.2. Static Clot

Porcine whole blood was drawn from the animal into several 25-35 mL syringes with 18G needles and immediately injected into IV tubing and six 100 mL plastic beakers. The tubing and beakers were left undisturbed at room temperature for 12 hr., then refrigerated at 4°C until testing. Additional 3 mL samples of citrated and EDTA whole blood were collected for determination of fibrinogen concentration and hematocrit.

### 2.3. Reconstituted Clot

Whole blood from swine was collected in CPDA1 donor bags (Baxter) and centrifuged at a relative centrifugal force of 2100g for 30 min. at 4°C. The plasma supernatant was heated to 53-56°C for 3 min., causing the fibrinogen to precipitate from solution<sup>14</sup>. Plasma fibrinogen was measured and determined to be <60 mg/dL (Beckman Electra 1600C Coagulation Analyzer). Porcine fibrinogen (Sigma, Fraction I) was added to a concentration of 300, 600 or 1,200 mg/dL. The separated erythrocytes and plasma were then recombined to a hematocrit of  $27 \pm 2\%$ . To form the reconstituted clot, 1000 US units of thrombin (bovine, Jones Pharma) (in 1 mL 0.9% saline with 40 mm  $\text{CaCl}_2$ ) was drawn into a 35 mL syringe followed by 34 mL of whole blood. This mixture was immediately injected into IV drip tubing or a 100mL plastic beaker and then incubated in a 37°C water bath for 1 hour.

### 2.4. Confined Compression Testing

35 mL samples of gelatin phantom, static clot or reconstituted clot in 100 mL plastic beakers were compressed under a solid cylindrical Delron plunger with a cross sectional area of 1,350 mm<sup>2</sup> (see Figure 1). This area was sized to match the inner diameter of the beaker with approximately 1 mm of space on each side. The samples were compressed at a rate of 25 mm/s. A 500 g load cell measured the force (in grams) and position (in  $\mu\text{m}$ ) every 5 ms. The force and position measurements were converted to stress (in kPa) and strain (change in length / original length). The slope of the linear region of the stress / strain curve was considered to be the compression modulus for each sample.

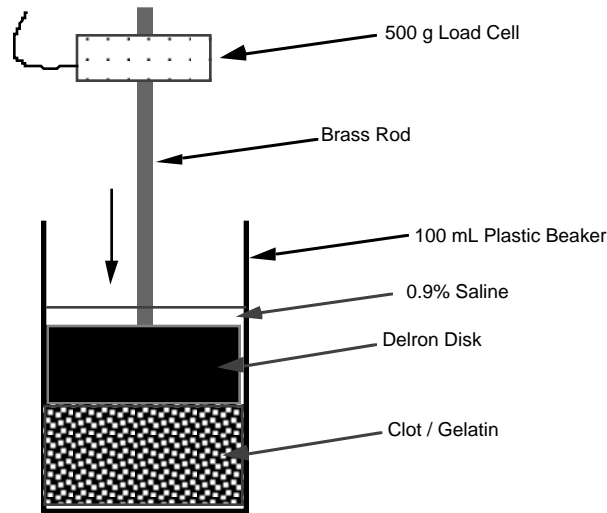


**Figure 1.** The confined compression set up. The gelatin or clot sample is formed in a 100 mL plastic beaker. Prior to testing, approximately 15 mL 0.9% saline is added. The Delron plunger is lowered to the surface of the sample, then pushed downward at a rate of 25 mm/s. A 500 g load cell measures the force (in grams) as the sample is compressed. Position (in  $\mu\text{m}$ ) is also monitored throughout the test.

## 2.5. Fluid Core Catheter

The 2 mm fluid core catheter contained a 200  $\mu\text{m}$  fiber in this study. The fluid core catheter acts as a conduit for the contrast dye (Hypaque 76, Nycomed) and the fiber. The 37°C contrast solution was injected at a rate of 4.2 mL/min.

## 2.6. Laser

The laser thrombolysis (ablation) experiments were performed with a Palomar 3010 pulsed dye laser emitting a 1  $\mu\text{s}$  pulse at 577 nm. The repetition rate was 4 Hz and the energy was approximately 25 mJ, producing an average power of 100 mW. Energy was measured before and after each experimental set. The average value of these two measurements was considered the effective energy.

## 2.7. Clot Ablation

A 30 mm section of tubing was cut and the clot or gelatin phantom was released into 0.9% saline. The clot was pulled into a 65 mm long section of silicone tubing (3 mm ID) which was inserted into the ablation chamber (see Figure 2). This internal diameter is equivalent to the diameter of vessels encountered in the clinical application. The fluid core catheter was advanced into the ablation chamber until the catheter tip was 1–2 mm from the proximal face of the clot. Contrast solution was injected for 30 sec. to build up to a 4.2 mL/min flow rate. Laser firing was performed for 30 seconds with simultaneous contrast injection. Following ablation, the proximal tubing was flushed with deionized water to remove all ablated fragments. Effluent was collected during the entire 1 min. experiment and flushing. Deionized water was added to each effluent sample to bring the total volume to 10 mL. Three control (contrast flow only) experiments were performed at the end of each experiment to account for mass removal due to mechanical forces from the contrast flow from the laser thrombolysis catheter system.

## 2.8. Spectrophotometry

Previous studies<sup>7,11</sup> have demonstrated that the absorbance of a solution at a given wavelength is directly proportional to its concentration. When the volume is held constant between samples, mass is equivalent to

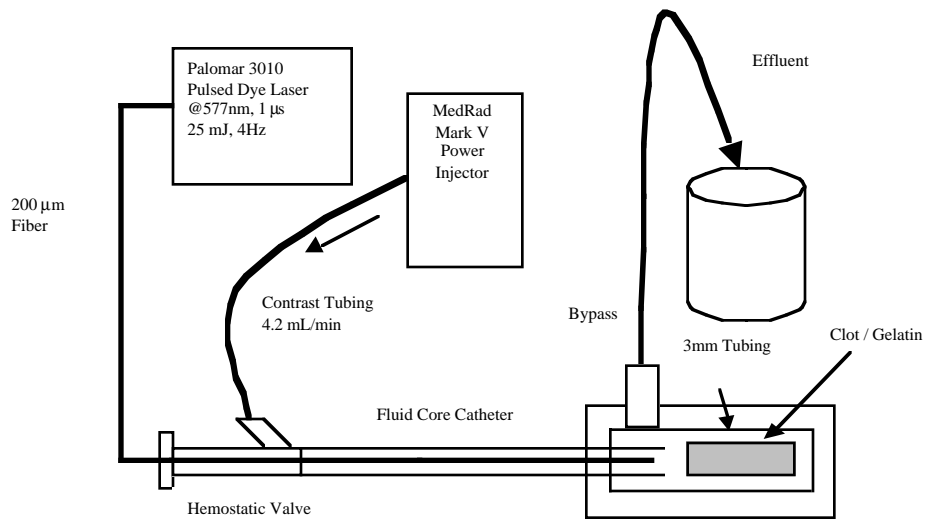


**Figure 2.** The *in vitro* laser thrombolysis experimental set up. Laser energy is delivered through the fluid core catheter to the clot in the ablation chamber. The ablation chamber contains a 3 mm inner diameter section of tubing that holds the clot and has a bypass for the collection of effluent.

Model	Hematocrit (%)	Fibrinogen (mg/dL)	$k$ ( $\text{g}^{-1}$ )	Laser Pulse Energy (mJ)
Gelatin	—	—	6.7	23.3
Static	26	309	141.6	25.0
Static	26	216	217.1	26.2
Static	26	200	215.9	27.8
Static	30	264	191.0	25.3
Reconstituted	28	300	201.3	25.3
Reconstituted	28	600	125.0	24.9
Reconstituted	28	1200	63.4	23.5

**Table 1.** Hematocrit, fibrinogen concentration, calibration factor  $k$ , and effective energy values for gelatin, static, and reconstituted clot models. The mean effective energy and range are reported for the gelatin models. Note that the gelatin phantom absorbance, and therefore  $k$ , was measured at 510 nm, while the static and reconstituted model clots were measured at 410 nm.

concentration. The mass of ablated clot or gelatin in an effluent sample can be determined by dividing the absorbance by a constant  $k$ . The relationship is summarized in the following equation:

$$\text{mass} = \frac{\text{Absorbance}(\lambda_{\text{peak}}) - \text{Absorbance}(800 \text{ nm})}{k}$$

where the constant  $k$  is experimentally determined and is equal to the slope of the graph of absorbance difference vs. mass. The hemoglobin in the reconstituted thrombus absorbs strongly at 410 nm; this wavelength provides the necessary sensitivity at the low concentrations of dissolved hemoglobin found in ablated samples. There is little absorbance by hemoglobin at 800 nm, therefore this wavelength was used as a baseline. Absorbance at 510 nm and 800 nm were measured for the gelatin / direct red samples. Dual wavelength spectroscopy was utilized to reduce error. This method was adapted from the method of Sathyam *et al.* (1996).

To generate a calibration curve, a range of clot or gelatin fragments similar in mass to those that would be produced in the ablation experiments were weighed to the nearest 0.01 mg in 50 mL beakers. 10 mL deionized water was added to each sample and the clot was mechanically and osmotically lysed. Gelatin samples were heated to melt the gelatin and liberate the dye. A 3 mL aliquot from each sample was measured with a spectrophotometer (HP 8425 Diode Array). Absorbance was measured at 410 (or 510) and 800 nm, and the difference was plotted against mass (See Figure 5). A linear curve fit was determined. The slope of this curve is the calibration constant  $k$  ( $\text{g}^{-1}$ ). The absorbance values were divided by the respective constant  $k$  to determine the mass ablation rate (in  $\mu\text{g}/\text{s}$ ) during each 30 sec. experiment.

## 2.9. Parameters

To test the effects of compression modulus on ablation efficiency ( $\mu\text{g}/\text{mJ}/\text{pulse}$ ), three clot models were tested. Gelatin with red dye was mixed in concentrations of 5, 10, 15, and 20% gelatin (wt/wt). Static clot was collected in a consistent manner from 4 swine. Three groups of reconstituted clots were made with fibrinogen concentrations of 300, 600, and 1,200 mg/dL. The normal range of fibrinogen in swine is 100–500 mg/dL<sup>15</sup>. The 300 mg/dL model clot therefore represents the median concentration, while the 600 mg/dL value was chosen since it was twice the median normal concentration. The 1,200 mg/dL represented a very strong clot (at 4 times the median *in vivo* value). The normal range of fibrinogen concentration in human plasma is 200-400 mg/dL, which supports the clinical relevance of this model.

## 3. RESULTS

### 3.1. Clot Parameters

The hematocrit and fibrinogen concentrations of the static and reconstituted model clots are listed in Table 1. The static clots all had fibrinogen concentrations within the normal range of 100–500 mg/dL. The mean hematocrit of the static clots was  $27 \pm 2\%$ . The hematocrits of the reconstituted model clots were intended to match this range.

### 3.2. Confined Compression Modulus

A typical stress / strain curve is shown in Figure 3. Stress is equal to the force (in grams)  $\times 9.81 \text{ m/s}^2$  (the acceleration of gravity) and the strain is calculated as the change in the length / the original length of the sample. The compression modulus is equal to the slope of the line fit to the data in the linear region of the stress / strain curve.

The mean compression modulus for each sample set is shown in Figure 4 and listed in Table 2. Error bars are 1 standard deviation. The % gelatin content and the fibrinogen concentration for static and reconstituted clots are shown. The modulus for the gelatin models ranged from 107-177 kPa and did not correlate with increases in gelatin content. The mean modulus for the static clots had the highest variability, both within and between groups and did not increase with fibrinogen concentration. There was no correlation between the fibrinogen content of the reconstituted model clots and their mean compression modulus, which ranged from 173-303 kPa.

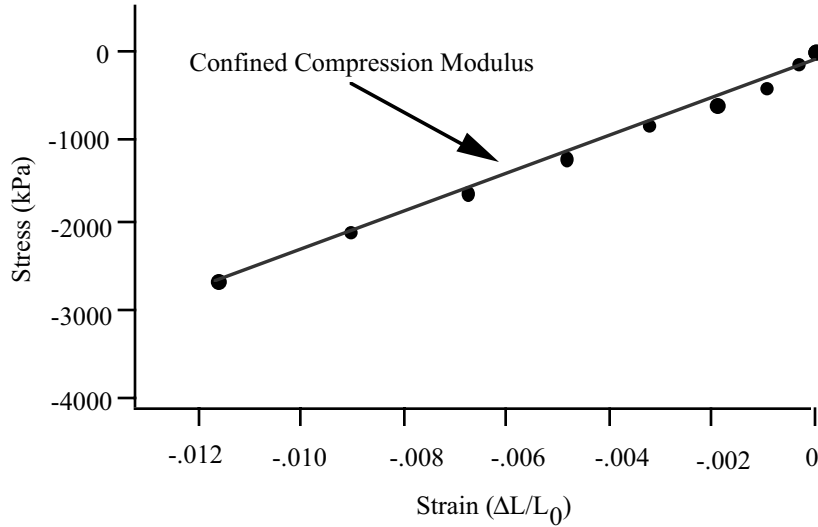


**Figure 3.** Typical stress/strain curve for a clot sample. The compression modulus is equal to the slope of the linear curve fit to the data.

### 3.3. Calibration Curves

A calibration curve (Figure 5) was plotted to determine the values of  $k$  at 410 nm for each static and reconstituted clot. The difference in absorbance at 410-800 nm vs. mass was graphed for each clot and a linear curve fit was determined. In this example,  $k=217.1 \text{ g}^{-1}$ . A single calibration curve at 510–800 nm was generated for the gelatin phantoms using the 10% gelatin sample. The range and mean  $k$  values for each model group are listed in Table 1.

### 3.4. Clot Ablation

The ablation efficiency of the gelatin models (in  $\mu\text{g}/\text{mJ}/\text{pulse}$ ) is inversely correlated to % protein (See Figure 6). The ablation efficiency of the static clot from the four swine was extremely variable between individuals. In contrast, the 300, 600, and 1,200 mg/dL reconstituted clots had similar mean ablation efficiency. The mean effective energy for each clot model group are listed in Table 1. The ablation efficiencies for each experiment was calculated by subtracting the control (contrast flow only) mass removed from the total mass removed and dividing this mass by the effective energy (mJ) and repetition rate (4Hz). The mean ablation efficiency and compression modulus for each group is summarized in Table 2. Figure 7 is a plot of ablation efficiency vs. compression modulus. There is no correlation between confined compression modulus and ablation efficiency in the range of stiffness tested in these three models.

## 4. DISCUSSION

Earlier gelatin phantom studies are consistent with our results, due to the homogeneity in strength and absorption coefficients between samples<sup>9</sup>. Detwiler *et al.* (1991) used a similar device to measure the unconfined compression modulus gelatin phantoms for their study on the effects of stiffness on mass removal of an ultrasonic angioplasty system<sup>16</sup>. They concluded that ultrasonic ablation decreased with increasing protein content of their gelatin target. These conclusions are supported by the current study of laser thrombolysis ablation of gelatin phantoms. Both ultrasonic angioplasty and the laser thrombolysis system under study remove target material through the formation and collapse of cavitation bubbles. The collapsing bubble generates a shock wave that is transmitted through the material, breaking it into smaller pieces. An important difference is that Detwiler measured unconfined compression, which is difficult to interpret, since fluid is allowed to escape from the sample during their test.

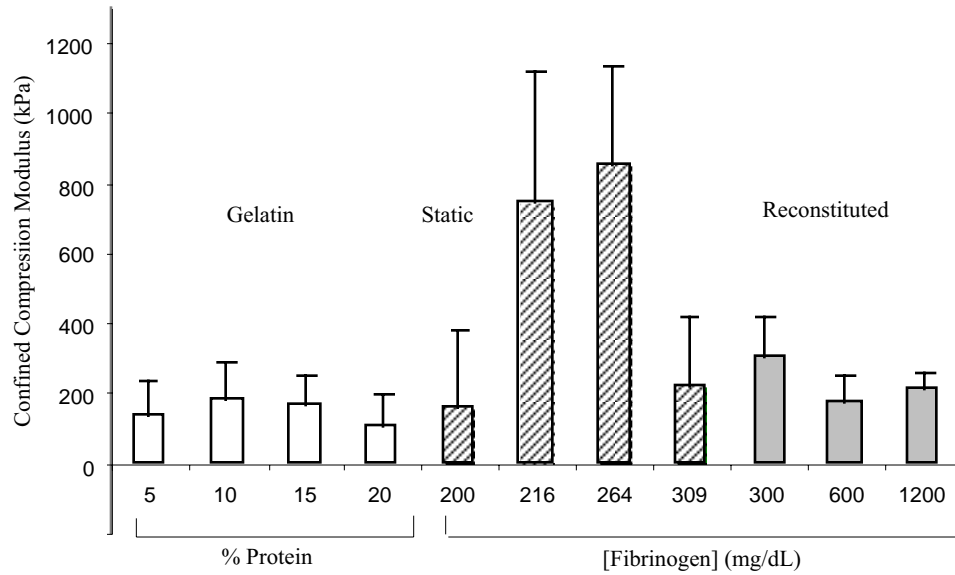


**Figure 4.** The mean confined compression modulus for each clot model. Gelatin samples are white, static clots are hatched, and reconstituted clots are gray. (N=6) for each set. Error bars are 1 standard deviation. Fibrinogen concentrations are given for the static and reconstituted model clots.

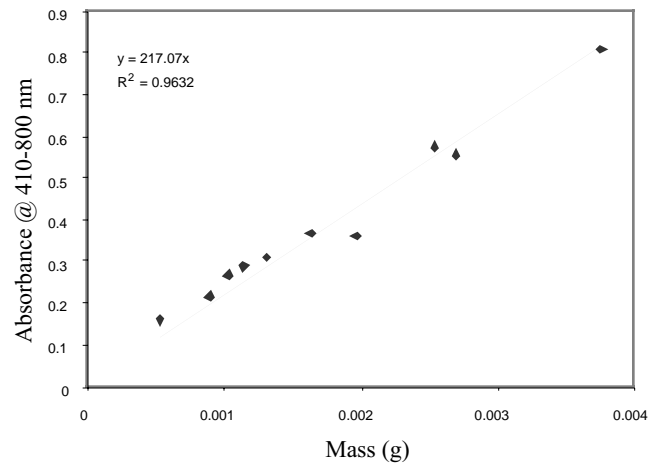


**Figure 5:** A typical calibration curve. Absorbance difference between 410 and 800 nm vs. mass, slope  $k=217.1 \text{ g}^{-1}$ .

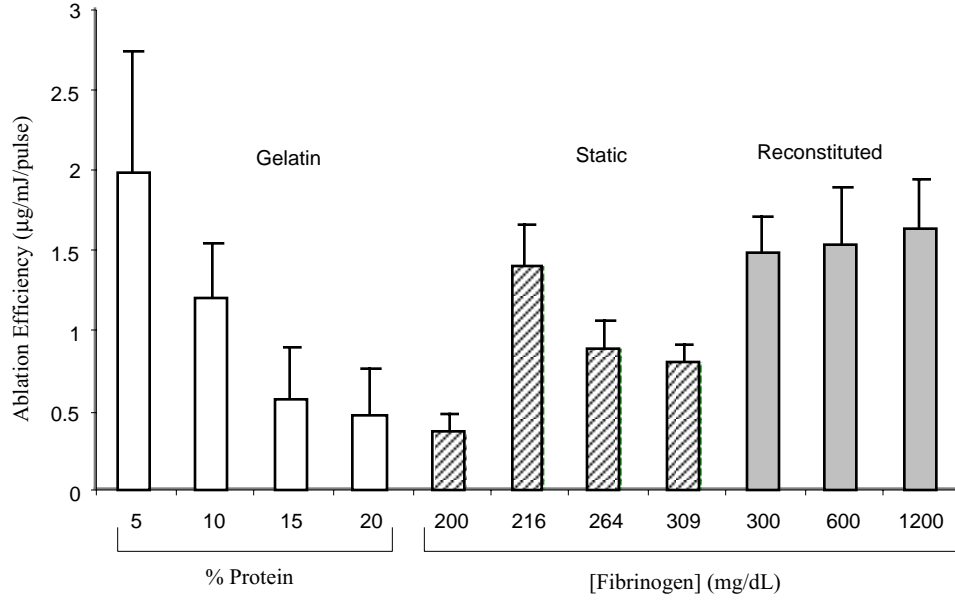


**Figure 6.** The mean ablation efficiency (in  $\mu\text{g}/\text{mJ}/\text{pulse}$ ) for each clot model. Gelatin samples are white, static clots are hatched, and reconstituted clots are gray. ( $N=10$ ) for each set. The mean control mass removal ( $N=3$ ) has been subtracted from each ablation efficiency. Error bars are 1 standard deviation. Fibrinogen concentrations are given for the static and reconstituted model clots.

Model	Fibrinogen Concentration (mg/dL)	Compression Modulus (kPa)	Ablation Efficiency ( $\mu\text{g}/\text{mJ}/\text{pulse}$ )
5% Gelatin	—	$140 \pm 90$	$2.0 \pm 0.7$
10% Gelatin	—	$180 \pm 110$	$1.2 \pm 0.3$
15% Gelatin	—	$160 \pm 190$	$0.6 \pm 0.3$
20% Gelatin	—	$110 \pm 80$	$0.5 \pm 0.3$
Static Clot	200	$160 \pm 220$	$0.4 \pm 0.1$
Static Clot	216	$750 \pm 370$	$1.4 \pm 0.3$
Static Clot	264	$850 \pm 280$	$0.9 \pm 0.2$
Static Clot	309	$210 \pm 210$	$0.8 \pm 0.1$
Reconstituted Clot	300	$300 \pm 120$	$1.5 \pm 0.2$
Reconstituted Clot	600	$170 \pm 80$	$1.5 \pm 0.3$
Reconstituted Clot	1,200	$210 \pm 60$	$1.6 \pm 0.3$

**Table 2.** The mean compression modulus and mean ablation efficiency  $\pm 1$  standard deviation for all model clots ablated. Gelatin phantoms are distinguished by the % protein; static and reconstituted clots are followed by the fibrinogen concentration in parentheses.



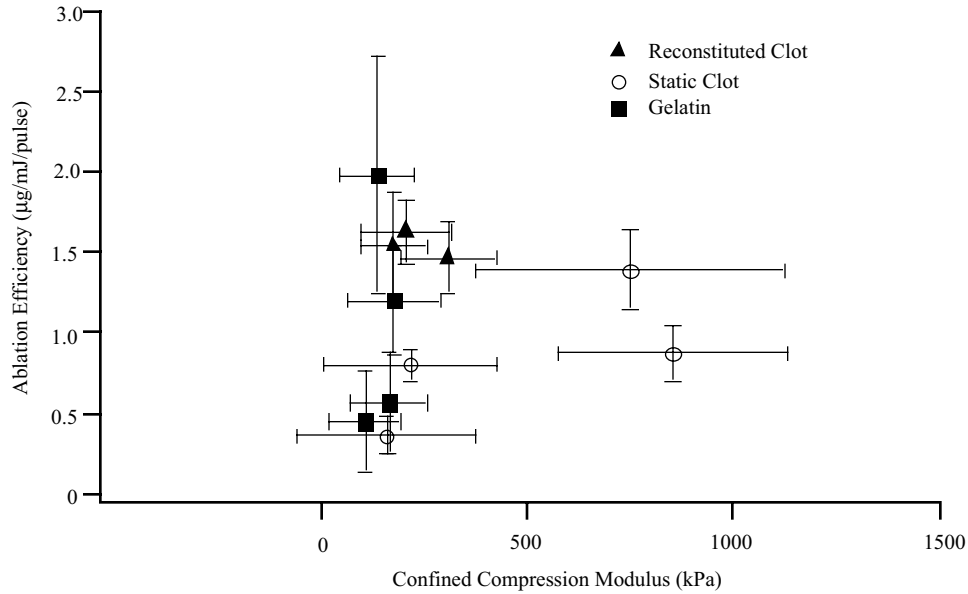


**Figure 7.** The mean ablation efficiency (in  $\mu\text{g}/\text{mJ}/\text{pulse}$ ). Gelatin samples are white, static clots are hatched, and reconstituted clots are gray. ( $N=10$ ) for each set. The mean control mass removal ( $N=3$ ) has been subtracted from each ablation efficiency. Error bars are 1 standard deviation. Fibrinogen concentrations are given for the static and reconstituted model clots.

The current study investigated the confined compression modulus of the three *in vitro* model clots. Because the fluid found within and around the sample is incompressible, confined compression allows more precise measurement of the properties of the solid under investigation. A fast rate of compression was eliminated stress/relaxation artifacts in this study. Additionally, compression modulus is affected by the rate of strain and cavitation bubble formation occurs at speeds greater than 1 m/s. The 25 mm/s strain rate used in these experiments was the best approximation of the high speed in cavitation that could be reliably produced by this mechanical tester.

This study demonstrates that the static clot model is too variable, both mechanically and in ablation experiments for reproducible *in vitro* testing of laser thrombolysis parameters. These experiments demonstrate equivalent ablation efficiency in model clots of similar confined compression modulus. (see Figures 4, 6, & 7). The reconstituted clots were not as stiff as two out of four of the static clots. This may be due to the activity of Factor XIII, which converts the fibrin-fibrin hydrogen bonds to stronger covalent bonds, in the static clot model. It was assumed that this enzyme is not active in the reconstituted model. The increases in fibrinogen content did not significantly affect the stiffness of the static or reconstituted clots, as measured by confined compression modulus. The differences demonstrated in the ablation of gelatin phantoms of varied protein content diminished the value of gelatin as a thrombus phantom. Gelatin is a suspension of partially denatured collagen molecules, while clot is held together by a meshwork of fibrin. These structural differences appear to have an effect on the ablation of the models.

Since the age of thrombus correlates with its mechanical properties *in vivo*<sup>17</sup>, these results support the use of laser thrombolysis for the removal of stroke causing clots of varying age and mechanical properties. The reconstituted clot model is a reproducible and clinically relevant *in vitro* target for bench top studies of laser thrombolysis.

The reconstituted clot model is histologically and ultrastructurally unique from clot formed *ex vivo*<sup>12</sup>. This is to be expected from a simplified clot phantom that lacks the complexity of the full hemostatic complement of enzymatic processes. However, the reconstituted clot model has easily manipulated optical and mechanical

strength properties. It is a more representative thrombus phantom than red gelatin because it consists of blood components, making it an ideal clot target for *in vitro* studies of laser thrombolysis.

## 5. CONCLUSIONS

The data demonstrates equivalent ablation efficiency (Figure 6) while varying model clot fibrinogen content. This provides some support for the use of the fluid core catheter system for the ablation of stroke causing clots of varied stiffness. The reconstituted clot model is a clinically relevant and reproducible *in vitro* target for the characterization of laser thrombolysis.

## ACKNOWLEDGEMENTS

Thank you to Lisa Welch for her assistance in obtaining the porcine blood. Additional thanks to Lisa Buckley for her work on the reconstituted clot model. This work was supported by LaTIS, Inc., Minneapolis, MN.

## 6. REFERENCES

1. Heart and Stroke Facts: 1996 Statistical Supplement. Dallas TX: American Heart Association, 1995.
2. Gregory KW , "Laser Thrombolysis" in Interventional Cardiology, vol 2. Topol EJ ed., Philadelphia:WB Saunders. pp 892-902, 1994.
3. Topaz O, Rosenbaum EA, Battista S, Peterson C, and Wysham DG, "Laser facilitated angioplasty and thrombolysis in acute myocardial infarction complicated by prolonged or recurrent chest pain," Cath. and Cardiovasc. Diag. 28, pp.7-16, 1993.
4. Topaz O and Vetrovec G, "Laser for optical thrombolysis and facilitation of balloon angioplasty in acute myocardial infarction following failed pharmacologic thrombolysis," Cath. and Cardiovasc. Diag. 36, pp. 38-42, 1995.
5. Gregory KW and Anderson RR, "Liquid core light guide for laser angioplasty," IEEE Quantum Electron. 26, pp. 2289-2296, 1990.
6. Gregory KW, Prince MR, LaMuraglia GM, Flotte TJ, Buckley L, Tobin JM, Ziskind AA, Caplin J, and Anderson RR, "Effect of blood upon the selective ablation of atherosclerotic plaque with a pulsed dye laser," Lasers Surg. Med. 10, pp. 533-43, 1990.
7. Sathyam U, Shearin A, Chastaney EA, and Prah SA, "Threshold and ablation efficiency studies of microsecond ablation of gelatin under water," Lasers Surg. and Med. 19, pp. 397-406, 1996.
8. Janis AD, Buckley LA, Gregory KW, "Laser thrombolysis in an *in vitro* model," Lasers in Surgery: Advanced Characterization, Therapeutics, and Systems X, Proceedings of SPIE Vol. 3907 (2000).
9. Shangguan H, Local Drug Delivery with Microsecond Laser Pulses: In Vitro Studies, PhD Thesis, Portland State University, Portland OR, 1996.
10. Viator JA and Prah SA, "Laser thrombolysis using long pulse frequency-doubled Nd:YAG lasers," Lasers Surg. and Med. 25, pp. 379-388, 1999.
11. Sathyam U, Laser Thrombolysis: Basic Ablation Studies, PhD Thesis, Oregon Graduate Institute of Science and Technology, Portland OR, 1996.
12. Janis AD, Nyara AN, Buckley LA, Gregory KW, "Characterization of an *in vitro* Laser Thrombolysis Model," Lasers in Surgery: Advanced Characterization, Therapeutics, and Systems XI, Proceedings of SPIE Vol. 4244 (2001).
13. Gelatin Manufacturers of Europe. Standardised Methods for the Testing of Edible Gelatins. Version 1. July 2000.
14. Prior JJ, Wallace DG, Harner A, Powers N, "A sprayable hemostat containing fibrillar collagen, bovine thrombin, and autologous plasma," Ann Thorac Surg 68, pp. 479-85, 1999.

15. Bowie EJ, Owen CA, Zollman PE, Thompson JH, Fass DN, "Tests of hemostasis in swine: Normal values and values in pigs affected with von Willebrand's disease," *Am J Vet Res* 34, pp. 1405-1407, 1973.
16. Detwiler PW, Watkins JF, Rose EA, Ratner AJ, Vu LP, Severinsky JY, Rosenschein U, "Mechanical and acoustic analysis in ultrasonic angioplasty," *Diagnostic and Therapeutic Cardiovascular Interventions, Proceedings of SPIE* Vol. 1425 (1991).
17. French JE. "The fine structure of experimental thrombi" in *Thrombosis*. Sherry S, Brinkhous KM, Genton E, and Stengle JE eds., Washington DC, National Academy of Sciences. pp. 300-320 (1969)